Investigation on Interfacial Adhesion Enhancement Mechanisms of TiAlN Coatings on Nitrocarburized 300M Steel

ZUO Shiwei[1], *LIANG Wenping*[2*], *MIAO Qiang*[2], *WU Hongyan*[3], *FAN Zhehang*[3], *GUO Huanyin*[4]

1. College of Mechanical and Electrical Engineering, Suzhou University, Suzhou 234000, P. R. China;
2. College of Materials Science and Technology, Nanjing University of Aeronautics and Astronautics, Nanjing 211106, P. R. China; 3. School of Chemistry and Materials Science, Nanjing University of Information Science and Technology, Nanjing 210044, P. R. China; 4. School of Information Engineering, Suzhou Vocational College of Civil Aviation, Suzhou 234000, P. R. China

(Received 2 July 2025; revised 23 September 2025; accepted 17 October 2025)

Abstract: This study investigates the interfacial adhesion enhancement mechanisms of TiAlN coatings deposited on nitrocarburized 300M ultra-high-strength steel substrates. Through radio frequency (RF) magnetron sputtering technology, TiAlN coatings (approximately 4 μm thick) are fabricated on both pristine and plasma-nitrocarburized (PNC) substrates. Comparative analyses of phase composition, microstructure, and mechanical properties are conducted using field emission scanning electron microscope (FESEM), X-ray diffraction(XRD), nanoindentation, and scratch testing. Molecular dynamics (MD) simulations with Materials Studio (MS) software elucidate atomic-scale interactions between TiAlN coatings and substrates. Results demonstrate that the PNC pretreatment generates a dual-phase structure (about 65 μm thick) comprising the γ-Fe_4N compound layer and a high-hardness diffusion layer, establishing a continuous hardness gradient at the coating-substrate interface. The PNC/TiAlN composite coating exhibits enhanced interfacial adhesion strength, attributed to mechanical interlocking from plasma-etched microvoids and optimized lattice matching. Scratch tests reveal a significant increase in critical load to 60 N for coating delamination in PNC/TiAlN systems compared with monolayer coatings. These improvements mitigate brittle spallation risks while maintaining superior hardness (29.26 GPa) and wear resistance. This paper provides atomic-level insights into adhesion enhancement mechanisms and proposes a viable duplex surface engineering strategy for high-strength steel components.

Key words: 300M steel; TiAlN coatings; nitrocarburized; interfacial adhesion strength

CLC number: TN925 **Document code:** A **Article ID:** 1005-1120(2025)06-0830-11

0 Introduction

300M steel is a low-alloy ultra-high-strength steel developed by the International Nickel Company (USA) in 1952. This alloy was engineered through the strategic incorporation of silicon (Si) and vanadium (V) as key modifying elements into the baseline AISI 4340 steel composition. 300M steel exhibits superior mechanical properties characterized by ultrahigh tensile strength, exceptional intrinsic fatigue strength, excellent fracture toughness, and outstanding resistance to stress corrosion cracking[1-2]. These advantages establish it as the globally recognized premier material for aircraft landing gear applications, delivering the highest achievable strength level coupled with optimal overall performance[3-4]. Since 1966, 300M steel has been extensively utilized as the primary landing gear material for both military and major commercial aircraft in the United States, including the Boeing

*Corresponding author, E-mail address: wpliang0905@163.com.

How to cite this article: ZUO Shiwei, LIANG Wenping, MIAO Qiang, et al. Investigation on interfacial adhesion enhancement mechanisms of TiAlN coatings on nitrocarburized 300M steel[J]. Transactions of Nanjing University of Aeronautics and Astronautics, 2025,42(6):830-840.

http://dx.doi.org/10.16356/j.1005-1120.2025.06.009

747, F-15, DC-10, and Boeing 707, accounting for over 90% of applications in this domain. China's research and development of low-alloy ultra-high-strength steel commenced in the 1970s, undergoing a transformative journey from initial imitation of foreign models to proprietary innovations, marked by progressive enhancement in material performance and manufacturing capabilities. During the early 1980s, a research team from the Materials Research Institute at Beijing University of Aeronautics and Astronautics initiated the reverse-engineering of 300M steel in compliance with the U.S. aerospace material standard AMS6417. This domestically developed alloy completed technical qualification in 1990 and was officially designated as 40CrNi2Si2MoVA[5-6]. To date, domestically produced 300M ultra-high-strength steel has been successfully applied to a series of indigenously-developed large aircraft including the J-15 carrier-based fighter, C919 passenger airliner, and Y-20 strategic transport aircraft. 300M steel exhibits a room-temperature yield strength exceeding 1 800 MPa and a tensile strength ranging from 1 860 MPa to 2 070 MPa[7]. Consequently, beyond its primary application in landing gears, this alloy is extensively utilized in critical aircraft components including fuselage frames, horizontal stabilizer shafts, and wing main spars, as well as large-scale load-bearing structural components in wind power and nuclear energy sectors[8-9]. Driven by technological advancements and the significant cost reduction achieved through the domestic production of 300M steel, this high-strength material has been widely adopted in critical structural components, notably including automotive engine housings, gears, and bearing components. Despite its extensive application in the aerospace industry, 300M steel remains susceptible to severe wear damage during service, posing significant risks to aircraft structural integrity. Consequently, substantial research efforts have been directed toward surface modification treatments to enhance its wear resistance, yielding promising outcomes in mitigating surface degradation mechanisms[10-12].

Physical vapor deposition (PVD) superhard coatings (e.g., TiN, CrN, and TiAlN), exhibiting superior hardness and elastic modulus, enable substantial enhancement in both the surface hardness and wear resistance of substrates[13-14]. Sahoo et al.[15] deposited different thicknesses (0.5, 1, 2 and 3 μm) TiAlN coatings onto WC micro-end mills via direct current magnetron sputtering. The coated tools exhibited a maximum microhardness of 34.8 GPa, demonstrating significantly enhanced wear resistance and mechanical properties compared with uncoated WC substrates. Yoon et al.[16] deposited TiN and TiAlN coatings on D2 steel substrates via multi-arc ion plating technique, both coatings had dense microstructures of approximately 2 μm in thickness. Comparative analysis revealed hardness values of 23 and 32 GPa for TiN and TiAlN coatings, respectively. Wear tests further demonstrated the superior wear resistance of TiAlN coatings, with this enhancement being particularly pronounced under high-speed machining conditions. However, although single-layer TiAlN coatings enhance hardness and wear resistance, their practical application is limited by delamination failure resulting from the coefficient of thermal expansion mismatch with steel substrates and inadequate interfacial adhesion. Plasma nitrocarburizing (PNC) pretreatment enables the formation of a high-hardness diffusion zone and compound layer (e.g., ε-$Fe_{2-3}N$) on the substrate surface[17]. This dual-phase structure not only enhances load-bearing capacity but also provides an optimized interfacial transition architecture for subsequent coatings[18]. Chen et al.[19] investigated the influence of nitrocarburizing pretreatment on PVD-deposited AlCrN coatings. The results demonstrated that the AlCrN coatings (approximately 2 μm thick) exhibited superior microhardness of approximately 43 GPa, while nitrocarburizing significantly enhanced the interfacial adhesion strength. Wang et al.[20] fabricated a PNC+CrN/CrTiAlSiN/WCrTiAlN composite coating on M420 steel substrates through sequential hollow cathode-assisted plasma treatment and multi-arc ion plating techniques. The comparative analysis revealed that the nitrogen-carbon diffusion layer effectively optimized

the hardness gradient at the coating-substrate interface, and the duplex-treated M420 stainless steel exhibited optimal corrosion resistance in natural seawater environments. Zuo et al.[21] successfully fabricated a PNC/TiAlSiN composite coating on 300M steel substrates via double glow plasma alloy technique and radio frequency (RF) magnetron sputtering equipment. The results demonstrated that the nitrocarburizing interlayer effectively suppressed brittle spallation of the TiAlSiN hard coating (approximately 6.5 μm thick), while maintaining superior wear resistance at elevated temperatures up to 400 ℃, and the composite system exhibited a significant enhancement in overall mechanical performance compared with monolayer TiAlSiN coatings. Therefore, introducing the nitrocarburizied layer is conducive to enhance the adhesion strength and frictional properties of super-hard coatings.

In the framework of this study, TiAlN coatings were deposited via magnetron sputtering technology on nitrocarburized substrates. A systematic analysis was conducted on the phase composition and mechanical properties of PNC/TiAlN composite coatings in comparison with monolayer TiAlN coatings. The interfacial bonding properties between the coating and substrate were critically analyzed from a molecular-level perspective using Materials Studio (MS) software, complemented by scratch testing to evaluate the interfacial adhesion strength of the samples. This study investigates the mechanical properties and adhesion characteristics of TiAlN coatings, aiming to further guide the better design of enhanced coating architectures.

1 Experiment

1.1 Specimen preparation

The substrate material employed in this experiment was 300M steel (40CrNi2Si2MoVA)[5], with its chemical composition detailed in Table 1. The material was sectioned into 16 mm × 14 mm × 5 mm specimens via laser cutting. These specimens were progressively ground using metallographic sandpaper up to 1 200 grit, followed by mechanical polishing and ultrasonic cleaning in acetone, prior to drying for subsequent use. The nitrocarburizing process utilized a honeycomb-structured graphite target (∅100 mm × 5 mm, 99.995% purity) supplied by Nanchang National Material Technology Co., Ltd., complying with ASTM C709-25 certification standards for ultra-high purity carbon materials. The TiAlN coating was deposited using a $Ti_{0.5}Al_{0.5}$ target material with 99.99% purity, measuring ∅100 mm × 5 mm, supplied by Beijing Hezong Tianqi Advanced Materials Co., Ltd.

Table 1 Chemical composition of 300M steel %

C	Si	Ni	Cr	Mn	Mo	V	Fe
0.43	1.64	1.85	0.80	0.79	0.39	0.08	Bal.

1.2 Preparation of modified coatings

Initially, selected specimens were subjected to nitrocarburizing treatment employing a dual-glow plasma surface alloying furnace manufactured by the Shenyang Scientific Instruments Co., Ltd., Chinese Academy of Sciences. The technical principles and operational methodology of this apparatus were detailed in Refs.[22-23]. The optimized processing parameters were configured as follows: workpiece bias voltage of 550 V, source voltage of 950 V, electrode spacing of 12 mm, working pressure of 30 Pa, Ar gas flow rate of 35 sccm, N_2 flow rate of 70 sccm, and holding time of 5.5 h. Subsequent heat treatments (including quenching and tempering) applied to the nitrocarburized substrates yielded a resultant hardness of 56-60 HRC, meeting standard industrial specifications. Subsequently, TiAlN coatings were simultaneously deposited onto both 300M steel substrates and the nitrocarburized specimens using a radio-frequency magnetron sputtering system produced by Shenyang Scientific Instrument Co., Ltd. of the Chinese Academy of Sciences. The optimized deposition parameters comprised: A target-to-substrate distance of 25 mm, applied power of 300 W, working pressure of 0.6 Pa, Ar flow rate of 30 sccm, N_2 flow rate of 90 sccm, deposition temperature of 350 ℃, and a dwell time of 3.5 h.

1.3 Characterization of coatings

A field-emission scanning electron microscope (FESEM, TESCAN-LYRA3, TESCAN ORSAY HOLDING a.s., Brno, Czech Republic) was used to examine the surface and cross-sectional morphology of the coatings and scratch tracks, as well as the energy-dispersive X-ray spectroscopy (EDS, XFlash® 6|60, Bruker Nano GmbH, Berlin, Germany) to determine their chemical composition. The crystallographic phases of the TiAlN coating were determined by grazing-incidence X-ray diffraction (GIXRD, Bruker D8 ADVANCE, Bruker AXS GmbH, Karlsruhe, Germany) using Cu Kα radiation, with an incidence angle of 1°, a scanning range from 20° to 90°, a scan rate of 1(°)/min, and a step size of 0.02°. The microhardness of the coatings were assessed through nanoindentation testing (Nanoindenter G200, Agilent Technologies Inc., Santa Clara, USA) system with a displacement loading rate of 10 nm/s and a maximum indentation load of 40 mN. The continuous stiffness measurement (CSM) method utilized a Berkovich diamond to penetrate the TiAlN coating, deriving hardness and modulus of elasticity based on the penetration depth, with a maximum indentation depth of t_{max} = 1 000 nm. In order to reduce the test error, three different positions of each sample were selected for testing, and the average value of relevant parameters was calculated. The interfacial binding energy between coatings and various substrates was calculated using the molecular dynamics (MD) module within MS software, elucidating the interfacial binding strength from an atomic-scale perspective. The interfacial adhesion strength between the coating and substrate was quantitatively characterized using a WS-2005 coating adhesion scratch tester. The testing protocol involved a progressive normal load ranging from 0 to 80 N applied to the diamond indenter, with a constant sliding velocity of 2 mm/min and a load application rate of 40 N/min. The resultant scratch track length was maintained at 4 mm for all measurements.

2 Results and Discussion

2.1 Microstructure and phases

Fig.1 displays the cross-sectional morphology of TiAlN coatings deposited on 300M steel substrate and nitrocarburized sample, respectively. To distinguish the cross-sectional morphologies between TiAlN and PNC/TiAlN samples, both specimens were etched for 10 s with a 4% nitric acid ethanol solution by volume fraction prior to SEM imaging (the etchant was prepared by mixing 4 ml of 65% analytical-grade nitric acid with 96 ml of anhydrous ethanol with purity ⩾99.7%). As shown from Fig.1, the TiAlN specimen comprises solely the TiAlN coating and the 300M steel substrate, whereas the PNC/TiAlN specimen consists of the TiAlN coating, a nitrocarburized layer, and the substrate. This configuration establishes a continuous hardness gradient from the surface to the substrate interior, thereby significantly enhancing the interfacial adhesion and wear resistance of the coating system. Fig.1(a) demonstrates a uniform and compact TiAlN coating intimately adhered to the 300M steel substrate, exhibiting a straight and distinct interface without detectable defects such as pores or cracks. As shown in Fig.1(b), the TiAlN coating exhibits a similarly uniform and dense microstructure, yet displays an irregular interface with the nitrocarburized substrate. This phenomenon primarily stems from the plasma etching-induced micro-voids formed on the substrate surface during the prior nitrocarburizing process. During subsequent TiAlN

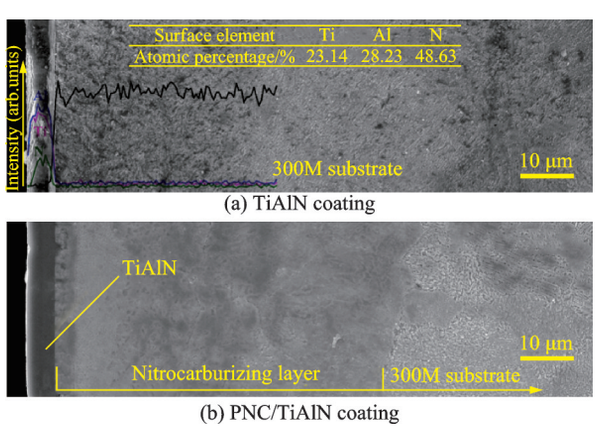

Fig.1 Cross-sectional morphologies of the TiAlN and PNC/TiAlN coatings

deposition, these micro-voids become infiltrated by the coating material, thereby establishing a mechanical interlocking effect. As documented, appropriately increased substrate surface roughness can significantly enhance the interfacial adhesion strength of hard coatings[24]. Both samples were co-deposited in the same furnace run under identical processing parameters, resulting in a uniform TiAlN coating thickness of approximately 4 μm for all specimens, and the thickness of nitrocarburized layer was about 65 μm. Additionally, the line scanning profile and surface elemental distribution of the TiAlN coating in Fig.1(a) reveal that Ti accounts for approximately 23% and Al for approximately 28%, with their peak intensities being comparable. In contrast, the N peak exhibits weaker intensity, which may primarily relate to its atomic mass. These results indicate that the elemental distribution is consistent with the formation of a (Ti, Al)N solid solution phase, though specific phase identification requires verification by XRD analysis.

Fig.2 presents the XRD patterns of 300M steel and PNC substrate, as well as TiAlN coatings with and without PCN treatments, which are used to analyze the phase structure of the materials. It is revealed that the 300M steel matrix and PNC matrix are predominantly composed of α-Fe and Fe_4N phases, respectively. Additionally, XRD analysis confirms that both TiAlN coatings consist exclusively of FCC (Ti, Al)N solid-solution phases. Characteristic diffraction peaks corresponding to the (200), (220), and (222) planes are observed at $2\theta = 35.8°$, 41.7°, and 60.3°, respectively. No detectable signatures of Ti-Al intermetallic compounds (e.g., Ti_3Al) or substoichiometric Ti_2N phases were observed within detection limits of conventional XRD. In contrast, the PNC/TiAlN coating system exhibits two distinct diffraction peaks at $2\theta = 43.6°$ (111) and 50.8° (200), corresponding to the Fe_4N phase. However, cross-referencing with the PDF database reveals that the diffraction angles of the AlN phase (PDF#: 25-1495) significantly overlap with those of the α-Fe phase (PDF#: 85-1410), complicating phase identification. Grazing-incidence XRD (GI-XRD) analysis of the TiAlN coating reveals potential α-Fe diffraction features; however, these signals are likely obscured by the dominant (Ti, Al)N peaks. Crucially, grazing-incidence XRD analysis definitively confirms that the observed diffraction features arise from the (Ti, Al) N solid-solution phase, rather than the substrate's α-Fe phase.

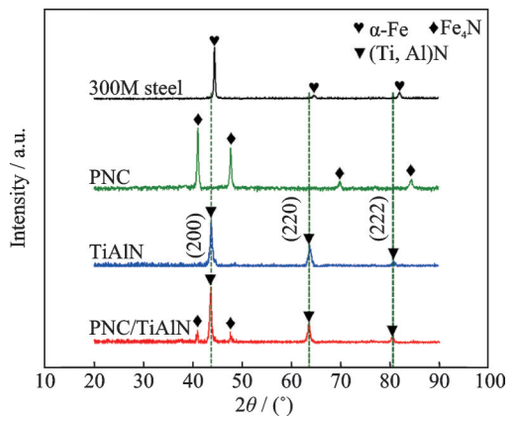

Fig.2 X-ray diffraction patterns for the 300M steel and PNC substrate, as well as TiAlN coatings with and without PCN treatments

2.2 Nanoindentation test

The wear resistance of materials exhibits a significant correlation with their hardness properties. This study utilizes nanoindentation testing to characterize the mechanical properties of TiAlN and PNC/TiAlN specimens. Comparative analysis reveals that the average hardness and Young's modulus values of the PNC/TiAlN coating are (29.26 ± 1.75) GPa and (272 ± 10) GPa, respectively, which are higher than those of the monolithic TiAlN coating ((26.73 ± 1.24) GPa and (245 ± 8) GPa, respectively), as shown in Fig.3(a). This enhancement is primarily attributed to the nitrocarburizing treatment, which significantly increases the substrate surface hardness, thereby providing enhanced resistance to plastic deformation for the outermost TiAlN layer.

To further investigate the hardness variation of TiAlN coatings along the depth direction, CSM was employed to test both samples, as shown in Fig.3(b). The results indicate that their initial-stage hardness values are nearly identical, and both exhibit a decreasing trend with increasing depth. However, the TiAlN coating exhibits a pronounced decline

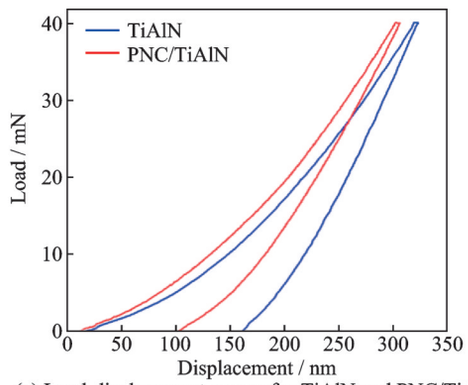

(a) Load-displacement curves for TiAlN and PNC/TiAlN

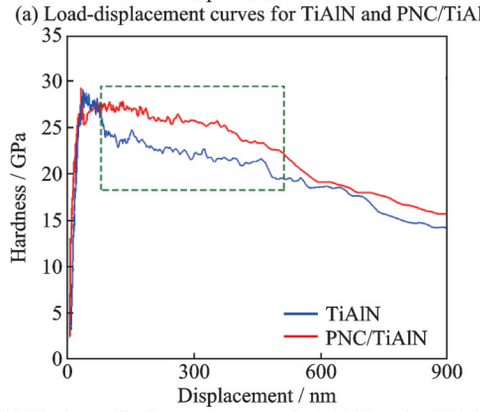

(b) Hardness-displacement curves for TiAlN and PNC/TiAlN

Fig.3 Nanoindentation test curves of TiAlN and PNC/TiAlN coatings

in hardness, indicative of its susceptibility to brittle spallation. In contrast, the hardness curve of the PNC/TiAlN sample demonstrates relatively stable behavior, with significantly higher hardness values observed within the 80—500 nm depth range compared with the TiAlN coating. This enhancement is primarily attributed to the plasma nitrocarburizing layer, which improves the continuity of hardness distribution and optimizes interfacial adhesion between the substrate and coating.

2.3 Interfacial adhesion strength analysis

Bonding strength serves as a critical mechanical property indicator for coatings, where robust interfacial adhesion fundamentally ensures their long-term service reliability. Current methodologies for characterizing coating-substrate bonding strength encompass tape adhesion tests, scratch tests, and Brinell indentation protocols. In this study, the interfacial bonding performance of TiAlN coatings was systematically evaluated through adsorption bonding analysis combined with scratch test methodology.

2.3.1 Analysis of bonding energy of TiAlN coating

During the deposition process of TiAlN coatings, localized peeling was occasionally observed in coatings fabricated on 300M steel substrates, as illustrated in Fig.4(a). In contrast, TiAlN coatings deposited on nitrocarburizing-treated surfaces showed no detectable interfacial failure features, as demonstrated in Fig.4(b). To address this, we propose a microscopic analysis of the aforementioned phenomenon. In the magnetron sputtering coating deposition process, the initial stage involves the adsorption of atoms on the solid surface, during which colliding atoms or molecules enter the transport zone between the gas phase and the substrate surface and undergo interactions[25-26]. In this study, the interfacial binding energy between coatings and different substrates was calculated utilizing the MD module in MS software, enabling further effective evaluation of the coating-substrate adhesion strength.

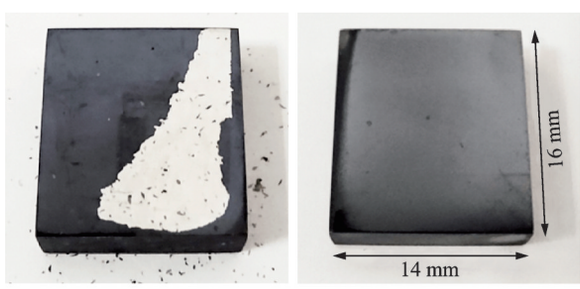

(a) TiAlN (b) PNC/TiAlN

Fig.4 Macroscopic morphology of TiAlN coatings prepared on surfaces of a 300M steel substrate and the nitrocarburizing diffusion layer

During the TiAlN coating deposition process via magnetron sputtering, Al and Ti atoms ejected from the target react individually with N atoms, ultimately depositing as AlN and TiN phases on the substrate surface. To streamline computational complexity, we characterized the interfacial bonding properties of TiAlN coatings deposited on different substrate surfaces using four representative models: AlN-Fe, TiN-Fe, AlN-Fe_4N, and TiN-Fe_4N. These models were systematically constructed through MS software, with their geometric configurations explicitly illustrated in Fig.5. During the

modeling process, the lattice parameters of the Fe, Fe_4N, AlN, and TiN crystalline phases, as listed in Table 2, were derived from corresponding XRD characterization results.

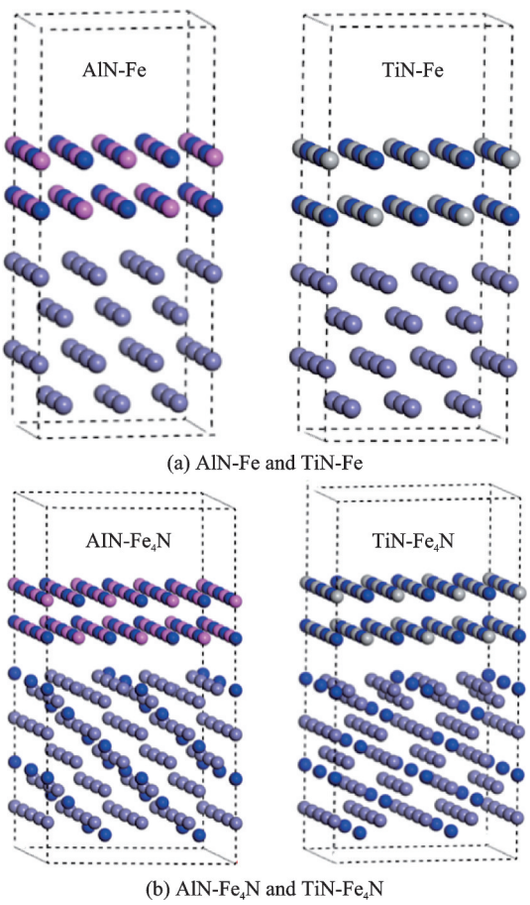

Fig.5 Structural models of AlN, TiN coatings with different substrates

Table 2 Lattice parameters of Fe, Fe_4N, AlN, and TiN phases

Phase	Lattice parameter
Fe	$a=b=c=0.286\ 6$ nm, $\alpha=\beta=\gamma=90°$
Fe_4N	$a=b=c=0.379\ 5$ nm, $\alpha=\beta=\gamma=90°$
AlN	$a=b=c=0.412\ 0$ nm, $\alpha=\beta=\gamma=90°$
TiN	$a=b=c=0.422\ 0$ nm, $\alpha=\beta=\gamma=90°$

Following the completion of model construction, the binding energy calculations for each configuration were performed using the MD module. Initial configurations were established with AlN and TiN positioned in ordered arrangements at approximately 0.351 nm from the substrate surface. The simulations reached equilibrium state after 250 000 computational steps, demonstrating stable energy convergence within the predefined threshold. The simulation results demonstrate that all AlN and TiN molecular models exhibit directional migration toward the substrate material. This dynamic process continues until the coating achieves complete encapsulation of the substrate surface and reaches thermodynamic equilibrium, with the final configuration explicitly illustrated in Fig.6.

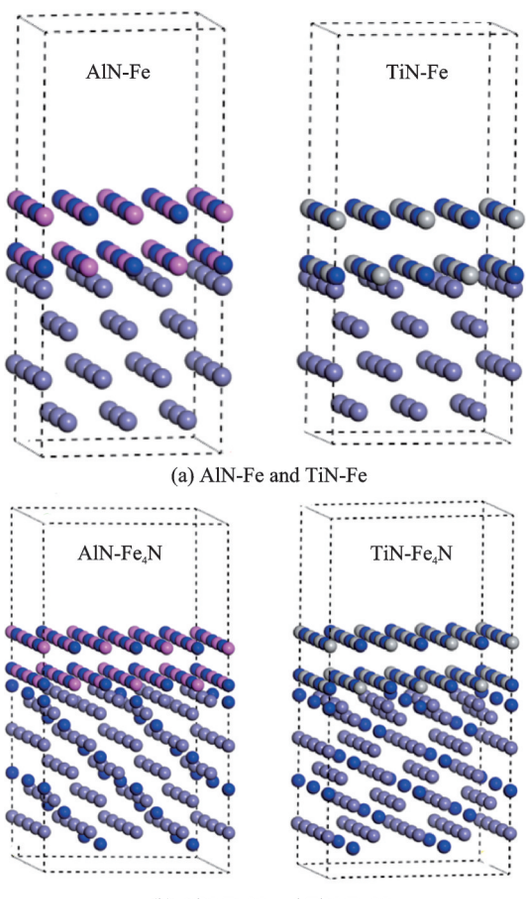

Fig.6 Structural models of AlN, TiN coatings with different substrates after simulating equilibrium

Generally, the dynamic behavior of molecular deposition can be elucidated by tracking the interaction binding energy of the system. The binding energy is estimated from the difference between the total potential energy of the system and the respective potential energies of the coating and substrate components[27-29], as specified in

$$\Delta E = E_{\text{total}} - (E_{\text{coating}} + E_{\text{substrate}}) \quad (1)$$

where E_{total} denotes the total potential energy of the coating system, E_{coating} the potential energy contribution from either the AlN or TiN coating layer, and

$E_{substrate}$ the potential energy of the Fe or Fe_4N substrate surface.

The computational results reveal negative ΔE values for all four investigated models, where a lower numerical value indicates stronger interfacial bonding energy between the coating and substrate. As shown in Fig.7, the ΔE values corresponding to AlN and TiN deposited on the Fe_4N substrate are significantly lower than those associated with the Fe substrate. This demonstrates that the TiAlN coating exhibits enhanced interfacial bonding strength when deposited on nitrocarburized substrate surfaces.

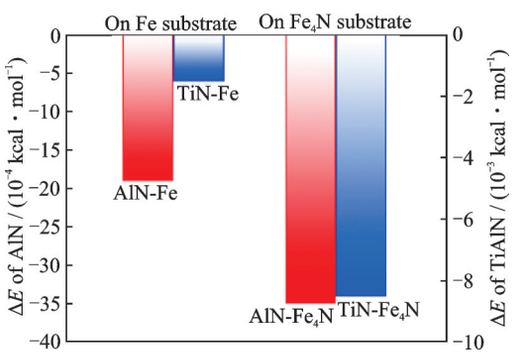

Fig.7 Distribution of ΔE values of AlN and TiN coatings deposited on Fe and Fe_4N substrates

2.3.2 Scratch test

The TiAlN and PNC/TiAlN scratch morphologies were shown in Fig.8. In scratch tests, Lc1 and Lc2 are critical indicators for evaluating the bonding strength between the coating and the substrate, representing the critical load for the initial failure occurrence and the critical load for complete coating failure, respectively. Experimental results unequivocally demonstrate that the TiAlN coating exhibits insufficient interfacial adhesion strength, as evidenced by extensive spallation initiation under a critical load (Lc2)[19] of approximately 15 N. This premature failure mechanism suggests critical limitations in coating-substrate adhesion under localized stress conditions. In contrast, the PNC/TiAlN sample demonstrated superior interfacial adhesion strength, exhibiting only localized coating delamination at the scratch terminus despite the presence of micro-cracks within the scratch track, and the quantitative analysis revealed an interfacial adhesion force exceeding 60 N. Firstly, the computational simulations conducted above demonstrate that the PNC/TiAlN coating exhibits significantly higher interfacial bonding strength compared with conventional TiAlN coatings; secondly, the nitrocarburizing treatment significantly enhances the surface hardness of the substrate, thereby providing superior resistance to plastic deformation for the outermost TiAlN coating. In other words, under identical deposition conditions, a higher substrate hardness correlates directly with a stronger interfacial bonding strength of the hard coating. Furthermore, the plasma nitrocarburizing process generates abundant fine particulate structures on the substrate surface, leading to an increased specific surface area. This morphological modification significantly enhances the adsorption capacity of the PNC-treated substrate for sputtered particles during the hard coating deposition, thereby contributing to improved mechanical properties of the resultant coating system.

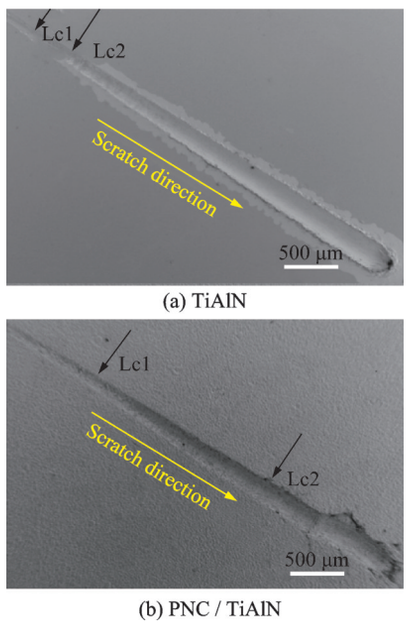

Fig.8 Scratch morphologies of the TiAlN and PNC/TiAlN coatings

3 Conclusions

This study demonstrates that the synergistic integration of PNC pretreatment and TiAlN coatings significantly enhances interfacial adhesion and mechanical performance in 300M ultra-high-strength

steel systems. Specifically, the PNC pretreatment generates a dual-phase structure comprising a high-hardness diffusion layer and a γ-Fe_4N compound layer, establishing a continuous hardness gradient from substrate to coating. The XRD and grazing-incidence analyses verify the exclusive presence of FCC (Ti, Al)N phases without deleterious intermetallic compounds, ensuring phase stability under operational stresses. Furthermore, MD simulations confirm substantially stronger interfacial bonding in PNC/TiAlN systems, where Fe_4N-terminated surfaces exhibit 1.8 — 4.7 times higher binding energies for AlN and TiN than that of Fe-substrate configurations, with optimized lattice matching reinforcing atomic-scale interactions. Finally, the average hardness and Young's modulus of the PNC/TiAlN coating are (29.26 ± 1.75) GPa and (272 ± 10) GPa, respectively, which are higher than those of the monolithic TiAlN coating. Concomitantly, the interfacial adhesion force is significantly increased to over 60 N, accompanied by superior resistance to brittle spallation during scratch testing. This duplex strategy provides atomic-level mechanistic insights for optimizing wear-resistant coatings on ultra-high-strength steels, with direct applicability to critical load-bearing components such as aerospace landing gears.

References

[1] ZHAO Mingjie, HUANG Liang, SUN Chaoyuan, et al. In-situ analysis on microstructure evolution of 300M steel during static holding process[J]. Acta Aeronautica et Astronautica Sinica, 2024, 45(18): 429734. (in Chinese)

[2] GAROIS S, DAOUD M, TRAIDI K, et al. Artificial intelligence modeling of induction contour hardening of 300M steel bar and C45 steel spur-gear[J]. International Journal of Material Forming, 2023, 16(3): 26.

[3] ZHENG Y S, LIU F G, GAO J Y, et al. Effect of different heat input on the microstructure and mechanical properties of laser cladding repaired 300M steel[J]. Journal of Materials Research and Technology, 2023, 22: 556-568.

[4] XIONG Y B, WEN D X, ZHENG Z Z, et al. Effect of heat treatment on microstructure and mechanical properties of directed energy deposition-arc 300M steel[J]. Materials Characterization, 2023, 198: 112756.

[5] GAO Y K, LI X B, YANG Q X, et al. Influence of surface integrity on fatigue strength of $40CrNi_2Si_2MoVA$ steel[J]. Materials Letters, 2007, 61(2): 466-469.

[6] LEPITRE P, MERLET L M, DOUDARD C, et al. Influence of shot-peening on the self-heating behavior and fatigue properties of 300M steel[J]. Mechanics of Materials, 2024, 199: 105174.

[7] LIU F G, LIN X, YANG H O, et al. Effect of microstructure on the fatigue crack growth behavior of laser solid formed 300M steel[J]. Materials Science and Engineering: A, 2017, 695: 258-264.

[8] ZUO S W, LI Q H, FAN Z H, et al. Influence of N_2 flow rate on mechanical and tribological properties of TAlN coatings deposited on 300M substrate and nitrocarburized layer[J]. Lubricants, 2025, 13(6): 254.

[9] DING W F, HAN M, ZHAO B, et al. Effects of intermittent cutting behavior on wear characteristics of alumina abrasive wheels during grinding ultra-high strength steels[J]. The International Journal of Advanced Manufacturing Technology, 2023, 129(5): 2801-2811.

[10] DANG J Q, LI Y G, ZHANG X X, et al. Surface fatigue characterization and its enhancement by the engineered ultrasonic rolling process for 300M ultrahigh strength steel[J]. Theoretical and Applied Fracture Mechanics, 2024, 134: 104707.

[11] ZHAO W D, LIU D X, HAO Z Q, et al. Improvement of corrosion and wear resistances of 300M ultra high strength steel by low temperature cathode assisted plasma nitriding[J]. Surface and Coatings Technology, 2024, 479: 130518.

[12] DONG Y A, LAN X Q, YANG S Q, et al. Effect of quenching and tempering treatments on microstructure and mechanical properties of 300M ultra-high strength steel fabricated by laser powder bed fusion[J]. Materials Characterization, 2024, 212: 113935.

[13] PAIVA J M, FOX-RABINOVICH G, LOCKS JUNIOR E, et al. Tribological and wear performance of nanocomposite PVD hard coatings deposited on aluminum die casting tool[J]. Materials, 2018, 11(3): 358.

[14] HEMMATI A, PAIVA J, VELDHUIS S C. Thermal stability and machining performance of arc evaporated $Ti_{1-x}Al_xN$ hard PVD coatings with x=0.5−0.73 ratios using an integrative approach[J]. Materialia, 2021, 17: 101132.

[15] SAHOO P, PATRA K. Cumulative reduction of friction and size effects in micro milling through proper selection of coating thickness of TiAlN coated tool: Ex-

perimental and analytical assessments[J]. Journal of Manufacturing Processes, 2021, 67: 635-654.

[16] YOON S Y, KIM J K, KIM K H. A comparative study on tribological behavior of TiN and TiAlN coatings prepared by arc ion plating technique[J]. Surface and Coatings Technology, 2002, 161(2/3): 237-242.

[17] DOU H C, ZHANG Z H, ZHANG M Y, et al. Tribological properties of the modified layers prepared on 38CrMoAl steel by plasma nitrocarburized and post-sulfurized method[J]. Vacuum, 2024, 228: 113473.

[18] ZHANG M M, ZHAI L, XUE Y, et al. Unusual intermediate layer precipitation in low-temperature salt bath nitrocarburized 316L austenitic stainless steel[J]. Surface and Coatings Technology, 2024, 494: 131521.

[19] CHEN W L, ZHENG J, MENG X N, et al. Investigation on microstructures and mechanical properties of AlCrN coatings deposited on the surface of plasma nitrocarburized cool-work tool steels[J]. Vacuum, 2015, 121: 194-201.

[20] WANG M F, LU J P, ZHOU Z L, et al. Corrosion studies of duplex surface-treated M420 stainless steel by plasma nitrocarburizing and WCrAlTiSiN multilayer coating[J]. Results in Surfaces and Interfaces, 2024, 16: 100230.

[21] ZUO S W, MIAO Q, LIANG W P, et al. A study on the mechanical performance and medium temperature tribological behavior of plasma nitrocarburizing/TiAlSiN/DLC composite coating[J]. Surfaces and Interfaces, 2021, 27: 101489.

[22] CUI S Y, MIAO Q, LIANG W P, et al. Oxidation behavior of NiCoCrAlY coatings deposited by double-Glow plasma alloying[J]. Applied Surface Science, 2018, 428: 781-787.

[23] ZUO S W, MIAO Q, LIANG W P, et al. Tribological studies of carbonitrided coatings synthesized on the 300M steels by double-glow plasma alloying[J]. Materials Research Express, 2019, 6(12): 126432.

[24] SHUM P W, ZHOU Z F, LI K Y. Friction and wear reduction of hard TiAlSiN coatings by an integrated approach of laser surface texturing and high-energy ion implantation[J]. Surface and Coatings Technology, 2014, 259: 136-140.

[25] ZHENG Weitao. Thin film materials and thin film technology[M]. Beijing: Chemical Industry Press, 2004. (in Chinese)

[26] ZHANG X Y, JIA B Y, ZENG Z, et al. Machine learning-based design of superhard high-entropy nitride coatings[J]. ACS Applied Materials & Interfaces, 2024, 16(28): 36911-36922.

[27] POGREBNJAK A D, KONG C H, WEBSTER R F, et al. Antibacterial effect of Au implantation in ductile nanocomposite multilayer (TiAlSiY)N/CrN coatings[J]. ACS Applied Materials & Interfaces, 2019, 11(51): 48540-48550.

[28] POGREBNJAK A D, WEBSTER R F, TILLEY R D, et al. Formation of Si-rich interfaces by radiation-induced diffusion and microsegregation in CrN/ZrN nanolayer coating[J]. ACS Applied Materials & Interfaces, 2021, 13(14): 16928-16938.

[29] GUO S W, LI L B, ZHANG G Y, et al. Adhesion analysis of electroless Ni coating on SiCp/Al composite mirror substrate[J]. Rare Metal Materials and Engineering, 2008, 37(6): 960-963.

Acknowledgements This work was supported by the National Major Science and Technology Projects of China (No. Y2022-Ⅲ-0004-0013), the National Natural Science Foundation of China (No. 52272065), the Sicence and Technology Plan Project of Suzhou City (N0. SZKXM202301), the Technical Service Project of Suzhou University (No. 2024xhx 140), the Suzhou University Doctoral Research Foundation (No. 2023BSK013), and the Natural Science Research Project in the Universities of Anhui Province (No. 2023AH053390).

Authors

The first author Dr. **ZUO Shiwei** received his B.S. degree in Inner Mongolia University of Technology, Hohhot, China, in 2014, M.S. degree in Inner Mongolia University of Science and Technology, Baotou, China, in 2016, and Ph.D. degree in Nanjing University of Aeronautics and Astronautics (NUAA), Nanjing, China, in 2022. From 2022 to present, he has been with College of Mechanical and Electrical Engineering, Suzhou University, Suzhou. His research is focused on plasma surface metallurgy, super-hard coating and friction and wear.

The corresponding author Prof. **LIANG Wenping** received her B.S. degree in Lanzhou University of Technology, Lanzhou, China, in 1986 and Ph.D. degree in Taiyuan University of Technology, Taiyuan, China, in 2007. From 2007 to present, she has been with College of Materials Science and Technology, NUAA. Her research field is plasma surface metallurgy, thermal barrier coating, environmental barrier coating, ultra-high temperature ceramic coating, etc.

Author contributions Dr. **ZUO Shiwei** designed the study, complied the models, conducted the analysis, interpreted the results, and wrote the manuscript. Prof. **LIANG**

Wenping and Prof. **MIAO Qiang** conceptualized the research objectives, supervised methodological validity, refined theoretical interpretations, and revised the manuscript critically. Prof. **WU Hongyan** contributed to the discussion and revision of the study. Mr. **FAN Zhehang** and Mr. **GUO Huanyin** contributed to the discussion and background of the study. All authors commented on the manuscript draft and approved the submission.

Competing interests The authors declare no competing interests.

(Production Editor: XU Chengting)

氮碳共渗300M钢表面TiAlN涂层界面结合增强机制研究

左士伟[1], 梁文萍[2], 缪　强[2], 吴红艳[3], 范哲航[3], 郭焕银[4]

(1.宿州学院机械与电子工程学院, 宿州 234000, 中国; 2.南京航空航天大学材料科学与技术学院,南京 211106, 中国; 3.南京信息工程大学化学与材料学院, 南京 210044, 中国; 4.宿州民航职业学院信息工程学院, 宿州 234000, 中国)

摘要:探讨了TiAlN涂层在氮碳共渗300M超高强度钢基体上界面结合性能增强的机理。采用射频(Radio frequency, RF)磁控溅射技术,在未经处理和经等离子体氮碳共渗(Plasma-nitrocarburized, PNC)处理的基体上分别制备了厚度约为4 μm的TiAlN涂层。通过场发射扫描电子显微镜(Field emission scanning electron microscope, FESEM)、X射线衍射(X-ray diffraction, XRD)、纳米压痕和划痕试验,对涂层的相组成、微观结构及力学性能进行了对比分析。利用Materials Studio软件进行分子动力学(Molecular dynamics, MD)模拟,阐明了TiAlN涂层与基体之间的原子尺度相互作用。结果表明:PNC预处理形成了由γ-Fe_4N复合层和高硬度扩散层组成的双相结构(约65 μm厚),在涂层-基体界面处形成了连续的硬度梯度;PNC/TiAlN复合涂层表现出增强的界面黏附强度,其机制可归因于等离子刻蚀微孔产生的机械互锁效应及优化的晶格匹配。划痕测试显示,相较于单层涂层,PNC/TiAlN体系的涂层剥落临界载荷显著提高至60 N。这些改进在保持优异硬度(29.26 GPa)和耐磨性的同时,降低了脆性剥落风险。本文从原子尺度解析了结合强度增强机制,并为高强钢构件提出了一种可行的复合表面工程方案。

关键词:300M钢;TiAlN涂层;氮碳共渗;界面结合强度